Quantification of Adventitial *Vasa Vasorum* Vascularization in Double-injury Restenotic Arteries

Meng Ye, Bai-Gen Zhang, Lan Zhang, Hui Xie, Hao Zhang

Department of Vascular Surgery, Ren Ji Hospital, School of Medicine, Shanghai Jiao Tong University, Shanghai 200127, China

Abstract

Background: Accumulating evidence indicates a potential role of adventitial *vasa vasorum* (VV) dysfunction in the pathophysiology of restenosis. However, characterization of VV vascularization in restenotic arteries with primary lesions is still missing. In this study, we quantitatively evaluated the response of adventitial VV to vascular injury resulting from balloon angioplasty in diseased arteries.

Methods: Primary atherosclerotic-like lesions were induced by the placement of an absorbable thread surrounding the carotid artery of New Zealand rabbits. Four weeks following double-injury induced that was induced by secondary balloon dilation, three-dimensional patterns of adventitial VV were reconstructed; the number, density, and endothelial surface of VV were quantified using micro-computed tomography. Histology and immunohistochemistry were performed in order to examine the development of intimal hyperplasia.

Results: Results from our study suggest that double injured arteries have a greater number of VV, increased luminal surface, and an elevation in the intima/media ratio (I/M), along with an accumulation of macrophages and smooth muscle cells in the intima, as compared to sham or single injury arteries. I/M and the number of VV were positively correlated ($R^2 = 0.82$, $P < 0.001$).

Conclusions: Extensive adventitial VV neovascularization occurs in injured arteries after balloon angioplasty, which is associated with intimal hyperplasia. Quantitative assessment of adventitial VV response may provide insight into the basic biological process of postangioplasty restenosis.

Key words: Angioplasty; Micro-computed Tomography; Restenosis; *Vasa Vasorum*

INTRODUCTION

Percutaneous transluminal angioplasty is important for the management of occlusive atherosclerotic lesions in humans. However, restenosis following angioplasty occurring in up to 50% of patients[1,2] limits the long-term effectiveness of this treatment. Postangioplasty restenosis pathophysiology has not been well-defined. Early studies to elucidate the mechanisms of restenosis focused on intimal de-endothelialization as a primary cause,[3] while more recent studies indicated a potential role for adventitial *vasa vasorum* (VV) in the initiation and/or progression of atherosclerotic lesions and vessel restenosis.[4-9] Adventitial VV is a network of microvasculature providing oxygen and nutrients to the outer layers of the arterial wall.[10,11] VV disruption may result in impaired oxygen transformation, vessel wall hypoxia, accumulation of oxidized metabolites, and nutritional deficiencies in the vessel wall.[12-15] VV can also serve as conduits for the recruitment of inflammatory cells, including macrophages, and noncellular inflammatory components.[16,17] These effects can lead to angiogenic and mitogenic factor expressions, including adhesion molecules and enzymes, in turn leading to smooth muscle cell (SMC) migration/proliferation, neointimal formation, vascular remodeling, and restenosis following angioplasty. Even though quantification of VV vascularization is reported in undiseased arteries following balloon overstretching,[18] responses of adventitial VV to angioplasty in severely diseased arteries, where angioplasty is normally performed in human patients, have not been examined or the relationship of these microvessels to changes in the intima. In the present study, we utilized a double-injury rabbit model: Primary lesions induced in carotid arteries by perivascular manipulation and balloon injury after 4 weeks. High-resolution three-dimensional (3D) volumetric data are suitable for the visualization and quantification of the entire VV microvasculature.[18] Micro-computed tomography (CT) has emerged as the preferred method for this purpose. In the present study, we used micro-CT combined with histological and immunobiochemistry methods to quantify the responses of VV and assess whether there is an association with neointimal formation in experimentally injured arteries following balloon dilation.

Address for correspondence: Dr. Hao Zhang,
Department of Vascular Surgery,
Ren Ji Hospital, Shanghai Jiao Tong University, 160 Pu Jian Road,
Shanghai 200127, China
E-Mail: chlzhcx@163.com

Methods

All animal procedures were reviewed and approved by the Institutional Animal Care and Use Committee at Shanghai Jiao Tong University medical division. Male New Zealand white rabbits (2.0–2.5 kg; 10–14 weeks old) were used in the present study. Two weeks prior to the first surgery, high cholesterol diet (2% cholesterol + 6% peanut oil + 92% normal chow diet) was begun in all animals, which was discontinued on the day of the second surgery (angioplasty) as previously described.[19] Animals were divided into three groups in order to demonstrate the various stages of vascular lesions: Group 1, sham operation group ($n = 6$) where animals underwent a sham operation; however, the artery was not impaired; Group 2, single-injury group induced by a constrictive thread loop ($n = 9$); and Group 3, double-injury group induced by angioplasty ($n = 10$).

Induction of the focal lesion in the right common carotid artery rabbits were anesthetized with 3% pentobarbital sodium using ear vein administration. Through a medial cervical incision, right common carotid arteries were exposed, and a 5–0 antibacterial (polyglactin 910) suture (Ethicon Ltd., Scotland, UK) was placed around the artery. Prior to ligation of the thread, a sterile metal tube with an external diameter of 0.7 mm was inserted in the suture collar parallel with the carotid artery, followed by withdrawal of the tube. Ampicillin (50 mg/kg) was administered intramuscularly (i.m.) immediately following surgical palliation.

Carotid angioplasty 4 weeks after focal carotid lesion induction, the right carotid artery was exposed, and the thread collar was found to be nearly completely absorbed in both single-injury and double-injury groups. Carotid angioplasty was performed in the double-injury group. Two vascular clips were placed on the carotid artery in order to prevent bleeding; one was placed onto the proximal common carotid artery, and the other was placed onto the internal carotid artery. A standard 3.0 mm × 17 mm percutaneous transluminal coronary angioplasty balloon was inserted in a retrograde fashion via the external carotid artery and was positioned at the point of ligation. For dilation, the balloon was inflated to six atmospheres for 2 min and then deflated and retracted, followed by ligation of the external carotid artery. All rabbits received a bolus of 100 μ/kg heparin intravenous (i.v.), and ampicillin (50 mg/kg) i.m.

Polymer injection and specimen dehydration after 4 weeks, all animals were sacrificed using a fatal dose (>100 mg/kg) of pentobarbital sodium, i.v. The right carotid was cannulated using a 2-mm-diameter plastic catheter. In order to clear the remaining blood from the carotid artery, we infused 500 ml of heparinized saline (0.9% sodium chloride containing 10,000 units of heparin) at 100 mmHg. We then infused low viscosity, radiopaque polymer compound (Microfil® MV-122, Flow Tech, Carver, MA, USA) through the catheter until the injected effluent flowed freely from the collateral common carotid vein. The tissues from each region were then removed from the neck and immersed in 10% neutral buffered formalin at 4°C overnight to polymerization occur. On the following day, the carotid artery was placed in 95% alcohol for 48 h. At 24-h intervals, the glycerin concentration was raised to 30%, 50%, 75%, and finally 100% glycerin in order to completely dehydrate the carotid segments. The specimen was then rinsed with acetone, left at room temperature for 24 h, and embedded in a paraffin mold for 3D micro-CT imaging.

Micro-CT imaging and reconstruction to preserve VV connectivity, the arteries were scanned in 2-cm increments along the arterial lumen axis without physically cutting the carotid artery. In the present study, the micro-CT scanner was configured so that the dimension of the cubic voxels was 20–25 μm (16-bit grayscale). The 3D images (an average number of 1000 slices per 2-cm carotid artery segment) were imaged using a high-resolution (8–36 μm isotropic voxel size) micro-CT imaging system (μCT80, Scanco Medical; Bassersdorf, Switzerland) and analyzed using the accompanying software.

Morphometric analysis

All specimens were traced, and cross-sections were analyzed at 2 mm intervals (excluding branching points) in order to yield 8–10 micro-CT cross-sections per 2-cm specimen. Vessel wall boundaries were defined using a radius of twice the distance from the arterial lumen to the outer adventitia. Blood vessels within this boundary were determined as VV. VV area within the vessel wall area was differentiated from nonvascular structures by setting the lower threshold values for an intensity range of interest that yielded the best identification of VV regions.

Two anatomically different types of VV have previously been defined.[18] First-order VV originated from the main carotid arterial lumen and ran longitudinally to the carotid artery. Second-order VV were smaller, and arose from branches of first-order, forming circumferential arches around the vessel wall. VV were manually counted and measured, and yielded the following morphometric variables for each cross-section: (a) VV density (VV per mm^2 vessel wall area) was calculated manually counting the VV and dividing by total area of the vessel wall; (b) the ratio of the number from second- to first-order VV; (c) the ratio of VV luminal volume (Volvv) to the total volume of contrast agent (Voltotal) within the arterial wall. VV luminal volume obtained was manually traced and measured on each cross-section, and (d) VV luminal surface fraction (the sum of VV luminal surface areas per mm^3 VolCA, mm^2/mm^3). The VV luminal surface area was calculated using the formula of the side surface area of a cylinder ($2 \times \pi \times$ radius × height).

Histological and immunohistochemical staining following micro-CT reconstruction and analysis, the specimens were immersed in 40°C water for 4 h to gently melt the wax embedding, followed by removal from the plastic mold and were cut every 2 mm. The sections were stained using Hematoxylin and Eosin (H and E) and elastic van Gieson

staining. The sections were then analyzed in order to determine the minimum luminal area (narrowest segment) for each carotid artery. This narrowest luminal area was at the level where the ligature was placed. Once the section with the smallest lumen from each vessel was determined, morphometric measurements for luminal, intimal, medial and total vascular areas were performed using digitized images of the van Gieson stained sections with a KS400 software package (Axioplan 2 imaging system).

In addition, immunohistochemical analysis was performed. A primary monoclonal antibody specific for vascular α-actin (MAB 1522, Chemicon International Inc.) was used at a dilution of 1:400 for the evaluation of vascular SMCs. For macrophage detection, a monoclonal antibody specific for rabbit macrophage CD68 (RAM 11, Dako) was diluted to 1:6500. The immunohistochemistry protocol has previously been described.[19] Briefly, sections were incubated with the primary antibody, anti-mouse IgG secondary antibody (biotin conjugate) and avidin peroxidase. The peroxidase was then visualized using chromagen. Sections were counterstained using H and E. A negative control was performed using primary antibodies replaced by mouse IgG isotype control in both α-actin and CD68 staining. The gray area of the stained section was analyzed. The unstained area was categorized as unclassified cell areas consisting of extracellular matrix and unstained cells.

Statistical analysis
All data are presented as mean ± standard error (SE). F-test was utilized to test for equality of variances among samples. One-way ANOVA, followed by a Tukey–Kramer *post-hoc* test with correction for multiple comparisons was used to identify statistical differences among the groups. Individual group comparisons were performed using an unpaired Student's *t*-test. Correlations among the continuous variables were analyzed by linear regression. $P < 0.05$ was considered as statistically significant.

RESULTS

Technical outcomes
All operative techniques were well-tolerated as suggested by normal food intake and normal movement. Three animals succumbed during this study. Because of the failure of wire traversing, two occluded arteries after primary injury were excluded from further study. Of the 30 rabbits initially studied, analyses were performed on 25 animals: 6 rabbits in sham operation group, 9 rabbits in primary lesion group and 10 rabbits in the balloon angioplasty model group.

Micro-computed tomography imaging
The carotid artery with a primary lesion showed a tendency for new vessel formation compared to sham, especially second-order VV with a shift toward second- to first-order VV [Figure 1 and Table 1] while no significant differences in VV luminal surface fraction or the ratio of Volvv to Voltotal were detected in these two groups [Table 1]. Four weeks following angioplasty, extensive neovascularization

of the adventitial VV with a profound shift in the ratio of second- to first-order VV was detectable, combined with a further decline in VV density [Figure 1 and Table 1] compared to sham. The VV luminal surface fraction and the Volvv to Voltotal ratio in the double-injury group were significantly elevated, compared to the sham and primary injury groups [Table 1].

Microscopic analysis
Animals subjected to constrictive thread placement showed mild formation of neointimal hyperplasia compared to sham. Morphometric analyses exhibited a significant elevation in intima/media ratio (I/M) 8 weeks following primary lesion [Figure 2a and 2b and Table 2]. At 4 weeks following balloon angioplasty, extensive intimal hyperplasia was developed with a high rate of I/M [Figure 2c and Table 2]. The thickened neointimal exhibited invasion of macrophages and accumulation of SMCs. The number of macrophages was mildly elevated in the single injury group (81.623 ± 13.240 vs. 70.944 ± 7.223 Grey/mm^2, $P = 0.043$, Figure 2d and e), coinciding with an increase in α-actin positive SMCs (228.933 ± 81.250 vs. 171.342 ± 28.52 n/mm^2, $P = 0.037$, Figure 2g and 2h) compared to sham. Following angioplasty, both macrophages (123.402 ± 5.121 vs. 70.944 ± 7.223 Grey/mm^2, $P = 0.014$, Figure 2f) and SMCs (352.167 ± 15.942 vs. 171.342 ± 28.523 n/mm^2, $P = 0.012$, Figure 2i) were significantly elevated.

Neointimal hyperplasia in histological sections with adventitial VV neovascularization assessed using cross-sectional micro-CT images demonstrated a positive correlation between I/M ratio and the number of VV in the angioplasty group ($R^2 = 0.82$, $P < 0.001$, Figure 3). Adventitial VV density declined in both the single- and double-injured groups [Table 1] as compared to sham. However, no significant correlation was observed between the I/M ratio and VV density.

DISCUSSION
This study was designed to identify the response of adventitial VV to acute vascular injury following angioplasty and examine potential associations with neointimal formation. Adventitial neovascularization and extensive intimal hyperplasia, characterized by accumulation of macrophages and SMCs, were detected using micro-CT and histology/immunohistochemistry in injured carotid arteries following balloon injury.

A rabbit model is commonly used to study responses to clinical angioplasty in a severely diseased artery.[20] In order to reproduce the morphological characteristics observed in patients who have undergone angioplasty, an initial injury must be induced in order to develop constrictive lesions, which will undergo angioplasty. The injury methods can include balloon injury,[21] wire loop,[22] air desiccation,[23] thermal drying,[24] or irradiation.[25] Recently, perivascular manipulation of the vessel wall using either placement
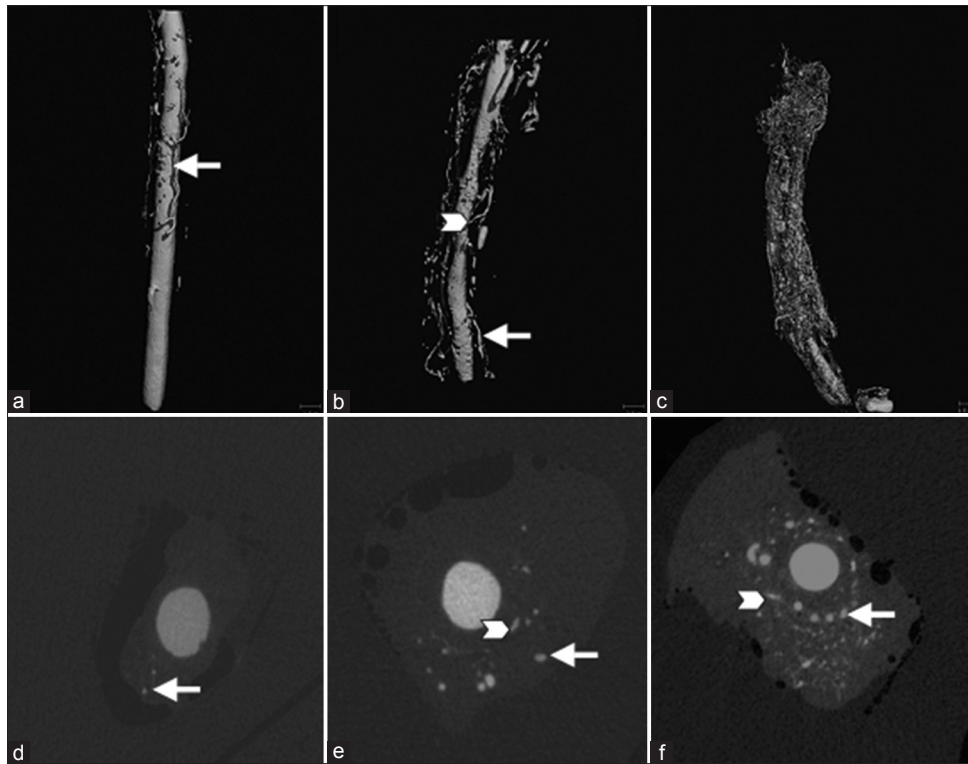
Figure 1: Top: Representative three-dimensional micro-computed tomography (CT) images of carotid arteries from the sham operation group (a), primary injury group (b), and angioplasty group (c). A denser plexus of microvessels in the adventitia was shown in the angioplasty group. Bottom: Representative cross-sectional micro-CT images of carotid artery from the sham operation group (d), primary injury (e) group and angioplasty group (f). Two anatomically different *vasa vasorum* (VV) types are identified: First-order VV (arrows) and second-order VV (arrowheads).

Table 1: Quantitative computerized digital analyses of micro-CT images

Items	Sham group ($n = 6$)	Single injury ($n = 9$)	Angioplasty ($n = 10$)	F	P
VV Number (n)	5.833 ± 0.477	7.429 ± 0.841	14.4 ± 1.176*†	21.374	0.000
VV density (n/mm²)	1.295 ± 0.110	0.927 ± 0.165*	0.857 ± 0.063*	4.074	0.033
Ratio 2nd/1st order VV	1.325 ± 0.371	1.784 ± 0.139	2.440 ± 0.214*	5.451	0.013
Volvv/Voltotal	0.176 ± 0.055	0.118 ± 0.035	0.326 ± 0.087†	2.728	0.094
VV endothelial surface fraction (VV endothelial surface areas/vessel wall volume mm²/mm³)	2.996 ± 0.689	2.794 ± 0.333	5.450 ± 0.799*†	5.424	0.015

*significantly different vs. sham operated group; †significantly different vs. single injury group. CT: Computed tomography; VV: *Vasa vasorum*; Volvv: VV luminal volume; Voltotal: the total volume of contrast agent.

of constrictive[26] or nonconstrictive cuffs around the vessel[27] or temporary ligation of the vessel[19] rapidly induced a focal atherosclerotic-like lesion, comprised of morphological changes in human atheroma. These alterations included macrophage and SMC infiltration into the arterial subendothelium, foam cell, cholesterol cleft, necrotic core, or fibrous capsule formation.

In the present study, we utilized a two-step injury model of the rabbit carotid artery, featuring a combination of a constrictive loop induced primary lesion and secondary balloon dilation. Manipulation of the outside of the rabbit right carotid artery accompanied by administration of a high cholesterol diet yielded mild intimal hyperplasia with increased densities of macrophage and SMC and decreases in lumen area[19,26,27] resembling features seen in early human atherosclerosis. Following the second injury that occurred

after balloon dilation, further remodeling of the carotid artery was evident with acute luminal dilatation, plaque fracture and extensive neointimal hyperplasia, reproducing the results of balloon angioplasty in human diseased vessels. We did not utilize the left carotid artery in the same animal with no balloon dilation as control, since after infusing and removing one side of artery for immediate fixation, it is difficult to maintain equal pressure to infuse the other artery. Lower pressure led to compromised resolutions in the micro-CT images and a reduced number of VV in the second infused artery, even following the first and second infused arteries in the same condition (data not shown). To avoid this bias, we used the first infused right carotid artery as our study vessel and compared across all groups.

Kwon *et al*.[18] reported results of arterial microcirculation following balloon injury in undiseased pig coronary arteries
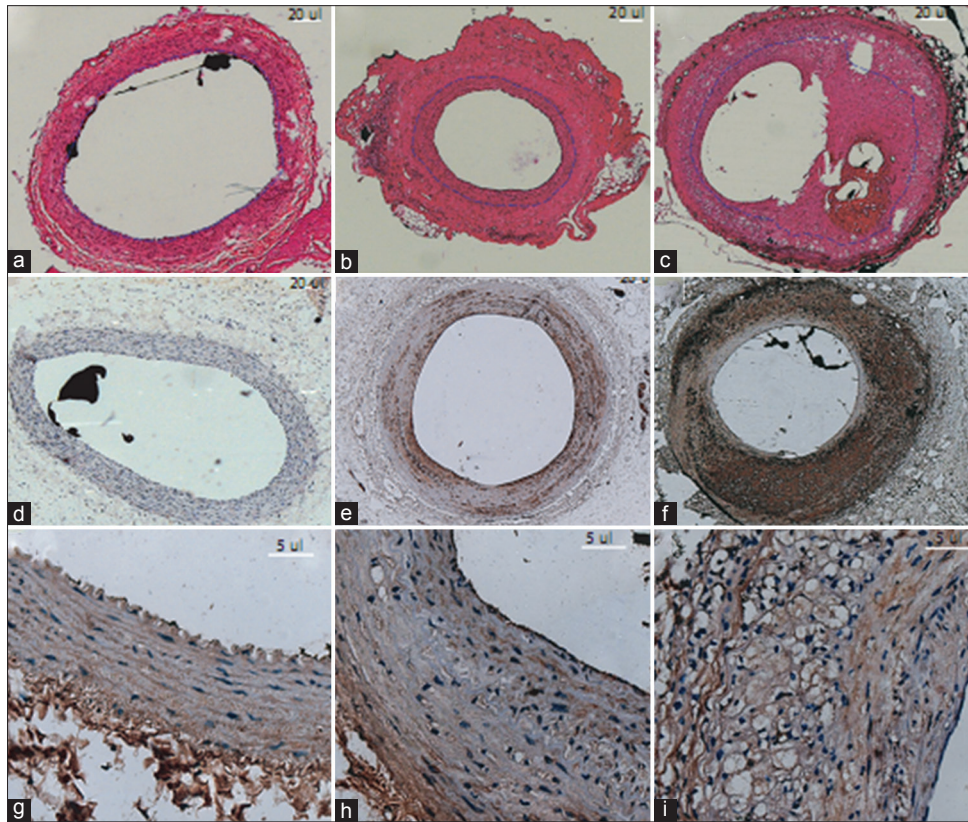
Figure 2: (a-c) Hematoxylin and Eosin staining of carotid arteries (×5). Mild intimal hyperplasia (surrounded by black dash line) was shown 8 weeks after absorbable suture was wrapped around the carotid artery (b). Pathologic intimal thickening with thrombotically active plaque was observed 4 weeks following balloon angioplasty (c). Arteriolar *vasa vasorum* (VV) filled with polymer (black) in sections; (d-f) Increased invasion of macrophages (brown) (×5) in single and double injury groups, revealed by monoclonal antibodies against macrophage marker CD68; (g-i) Accumulation of smooth muscle cells (×40) in injury groups. Spindle-shaped smooth muscle cells were brown in color with long nuclei stained dark blue.

Table 2: Cross-sectional area of rabbit carotid arteries at the narrowest segment

Items	Sham group (n = 6)	Single injury (n = 9)	Angioplasty (n = 10)	F	P
Lumen	0.794 ± 0.126	0.660 ± 0.039	1.052 ± 0.015	1.735	0.201
Intima	0.070 ± 0.011	0.500 ± 0.105	1.006 ± 0.172*†	9.437	0.001
Media	0.388 ± 0.037	0.561 ± 0.085	0.739 ± 0.049*†	5.140	0.015
I/M	0.179 ± 0.023	0.885 ± 0.194*	1.400 ± 0.238*	7.609	0.003

*significantly different vs. sham operated group; †significantly different vs. single injury group. I/M: Intima/media ratio.

using micro-CT. These investigators observed that the number of VV vessels, especially in second-order VV, was increased in the injured vessel. The density of newly formed vessels was also increased, correlating with vessel stenosis. In our current study, we observed a similar response of VV neovascularization with significantly increased second-order VV in experimentally injured carotid arteries after balloon angioplasty. New VV vessels were proportional to intimal hyperplasia. Notably, mild VV neovascularization and neointimal hyperplasia were detected in carotid arteries following primary injury. These vessels may serve as further neovascularization following angioplasty-induced injury.

Despite increases in the total number, we have shown that the density of newly formed VV was decreased in injured arteries following balloon dilation. The difference in VV density between Kwon *el al*.[18] and our studies may likely reflect difference in the stage of restenosis. In the present study, we evaluated restenosis at an early phase, as indicated by a lack of the severe intimal hyperplasia, the surface of the lumen was larger than sham. It is possible that the 4-week time point is not sufficient and a longer period may be necessary for complete remodeling of the injured area and restenosis. Low VV densities after balloon dilation can cause hypoxia, oxidative stress and microflammation in the balloon-injured artery wall, which could lead to intimal growth. This is supported by micro-CT results of Gössl *et al*.[28] These authors found that the areas of low VV densities within coronary arteries show decreased oxygenation and increased oxidative stress, which can cause microinflammation and subintimal proliferation and potentially initiate the early atherosclerosis development. It is possible that angiogenic stimulation to enhanced VV neovascularization during the early phase of acute vessel injury can reduce intimal hypoxygen by an increased oxygen supply. Kwon *et al*.[18] showed a potential for advanced restenosis, as the artery lumen stenosis was about 45% following balloon injuries.[18] Although VV neovascularization can serve as a compensatory mechanism for the delivery of more oxygen and nutrients to injured vessel walls for vascular repair during the advanced stage of restenosis, higher densities of VV may actually aggravate the
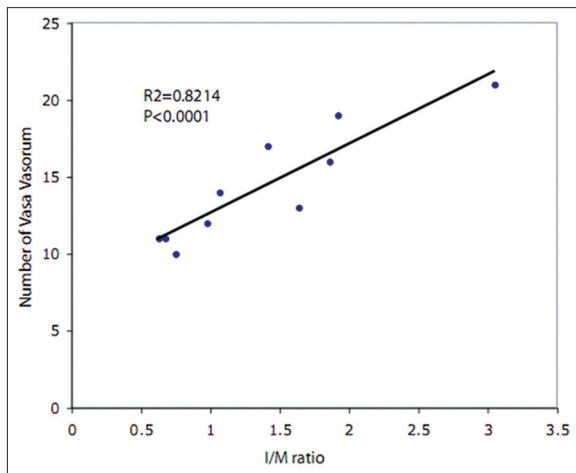
Figure 3: Correlation between histology and based intima/media ratio and the number of vasa vasorum in the angioplasty group ($n = 10$).

restenosis. This could function as a conduit for macrophages or inflammatory factor infiltration that could promote the progression of inflammation and restenosis formation. This is supported by Moulton *et al.*[17] who showed that inhibition of VV neovascularization reduced macrophage accumulation and progression of atherosclerotic plaques. Indeed, along with increased VV formation, the invasion of macrophages was detected in the primary atherosclerotic group and was further enhanced following balloon injury. Two aspects of VV neovascularization in the progression of restenosis may explain why some studies showed that angiogenic cytokines can accelerate reendothelialization, improve endothelial function, and significantly reduce intimal proliferation in models of balloon-induced arterial injury,[29,30] while other studies have shown that angiogenic cytokines can accelerate atherogenesis.[16,31] Further experimental studies are required in order to better understand of the right timepoint for both angiogenesis and anti-angiogenesis/anti-inflammation therapy in order to reduce arterial restenosis.

We found that the luminal surface of VV was higher in the double injured angioplasty group, compared to the sham and primary injury groups. This could indicate elevated exchange between cellular and noncellular components and the vascular wall. This could allow more oxygen and nutrition transported into the vessel wall, which could enhance arterial repair following acute injury. Alternatively, it could promote intimal hyperplasia and restenosis, as newly formed VV are considered to be more fragile, leaky and more prone to rupture.[5]

In conclusion, The double-injury rabbit model of restenosis coupled with perivascular manipulation and secondary balloon injury closely mimics human disease. Marked VV neovascularization occurred in rabbit carotid arteries following balloon injury. The number of VV was increased proportionally to intimal hyperplasia while VV density was decreased in the injured arteries. Additional studies are required to determine whether modifying VV growth could provide therapeutic effects on neointimal hyperplasia and restenosis following arterial injury.

References

1. Smith SC Jr, Dove JT, Jacobs AK, Kennedy JW, Kereiakes D, Kern MJ, *et al.* ACC/AHA guidelines for percutaneous coronary intervention (revision of the 1993 PTCA guidelines)-executive summary: A report of the American College of Cardiology/American Heart Association task force on practice guidelines (Committee to revise the 1993 guidelines for percutaneous transluminal coronary angioplasty) endorsed by the Society for Cardiac Angiography and Interventions. Circulation 2001;103:3019-41.
2. Teirstein PS. Living the dream of no restenosis. Circulation 2001;104:1996-8.
3. Clowes AW, Clowes MM, Fingerle J, Reidy MA. Kinetics of cellular proliferation after arterial injury. V. Role of acute distension in the induction of smooth muscle proliferation. Lab Invest 1989;60:360-4.
4. Barker SG, Talbert A, Cottam S, Baskerville PA, Martin JF. Arterial intimal hyperplasia after occlusion of the adventitial vasa vasorum in the pig. Arterioscler Thromb 1993;13:70-7.
5. Barger AC, Beeuwkes R 3rd, Lainey LL, Silverman KJ. Hypothesis: Vasa vasorum and neovascularization of human coronary arteries. A possible role in the pathophysiology of atherosclerosis. N Engl J Med 1984;310:175-7.
6. Williams JK, Armstrong ML, Heistad DD. Vasa vasorum in atherosclerotic coronary arteries: Responses to vasoactive stimuli and regression of atherosclerosis. Circ Res 1988;62:515-23.
7. Shi Y, Pieniek M, Fard A, O'Brien J, Mannion JD, Zalewski A. Adventitial remodeling after coronary arterial injury. Circulation 1996;93:340-8.
8. Scott NA, Cipolla GD, Ross CE, Dunn B, Martin FH, Simonet L, *et al.* Identification of a potential role for the adventitia in vascular lesion formation after balloon overstretch injury of porcine coronary arteries. Circulation 1996;93:2178-87.
9. Staab ME, Srivatsa SS, Lerman A, Sangiorgi G, Jeong MH, Edwards WD, *et al.* Arterial remodeling after experimental percutaneous injury is highly dependent on adventitial injury and histopathology. Int J Cardiol 1997;58:31-40.
10. Werber AH, Heistad DD. Diffusional support of arteries. Am J Physiol 1985;248(6 Pt 2):H901-6.
11. Geiringer E. Intimal vascularization and atherosclerosis. J Pathol Bacteriol 1951;63:201-11.
12. Järvilehto M, Tuohimaa P. Vasa vasorum hypoxia: Initiation of atherosclerosis. Med Hypotheses 2009;73:40-1.
13. Pugh CW, Ratcliffe PJ. Regulation of angiogenesis by hypoxia: Role of the HIF system. Nat Med 2003;9:677-84.
14. Rodriguez-Porcel M, Lerman LO, Holmes DR Jr, Richardson D, Napoli C, Lerman A. Chronic antioxidant supplementation attenuates nuclear factor-kappa B activation and preserves endothelial function in hypercholesterolemic pigs. Cardiovasc Res 2002;53:1010-8.
15. Yun AJ, Doux JD, Bazar KA, Lee PY. Adventitial dysfunction: An evolutionary model for understanding atherosclerosis. Med Hypotheses 2005;65:962-5.
16. Moulton KS, Heller E, Konerding MA, Flynn E, Palinski W, Folkman J. Angiogenesis inhibitors endostatin or TNP-470 reduce intimal neovascularization and plaque growth in apolipoprotein E-deficient mice. Circulation 1999;99:1726-32.
17. Moulton KS, Vakili K, Zurakowski D, Soliman M, Butterfield C, Sylvin E, *et al.* Inhibition of plaque neovascularization reduces

macrophage accumulation and progression of advanced atherosclerosis. Proc Natl Acad Sci U S A 2003;100:4736-41.

18. Kwon HM, Sangiorgi G, Ritman EL, Lerman A, McKenna C, Virmani R, *et al.* Adventitial vasa vasorum in balloon-injured coronary arteries: Visualization and quantitation by a microscopic three-dimensional computed tomography technique. J Am Coll Cardiol 1998;32:2072-9.

19. Leidenfrost JE, Khan MF, Boc KP, Villa BR, Collins ET, Parks WC, *et al.* A model of primary atherosclerosis and post-angioplasty restenosis in mice. Am J Pathol 2003;163:773-8.

20. Touchard AG, Schwartz RS. Preclinical restenosis models: Challenges and successes. Toxicol Pathol 2006;34:11-8.

21. Sarembock IJ, LaVeau PJ, Sigal SL, Timms I, Sussman J, Haudenschild C, *et al.* Influence of inflation pressure and balloon size on the development of intimal hyperplasia after balloon angioplasty. A study in the atherosclerotic rabbit. Circulation 1989;80:1029-40.

22. Reidy MA, Schwartz SM. Endothelial regeneration. III. Time course of intimal changes after small defined injury to rat aortic endothelium. Lab Invest 1981;44:301-8.

23. Fishman JA, Ryan GB, Karnovsky MJ. Endothelial regeneration in the rat carotid artery and the significance of endothelial denudation in the pathogenesis of myointimal thickening. Lab Invest 1975;32:339-51.

24. Douek PC, Correa R, Neville R, Unger EF, Shou M, Banai S, *et al.* Dose-dependent smooth muscle cell proliferation induced by thermal injury with pulsed infrared lasers. Circulation 1992;86:1249-56.

25. Fajardo LF, Berthrong M. Vascular lesions following radiation. Pathol Annu 1988;23(Pt 1):297-330.

26. Jahnke T, Karbe U, Schäfer FK, Bolte H, Heuer G, Rector L, *et al.* Characterization of a new double-injury restenosis model in the rat aorta. J Endovasc Ther 2005;12:318-31.

27. Booth RF, Martin JF, Honey AC, Hassall DG, Beesley JE, Moncada S. Rapid development of atherosclerotic lesions in the rabbit carotid artery induced by perivascular manipulation. Atherosclerosis 1989;76:257-68.

28. Gössl M, Versari D, Lerman LO, Chade AR, Beighley PE, Erbel R, *et al.* Low vasa vasorum densities correlate with inflammation and subintimal thickening: Potential role in location – Determination of atherogenesis. Atherosclerosis 2009;206:362-8.

29. Asahara T, Chen D, Tsurumi Y, Kearney M, Rossow S, Passeri J, *et al.* Accelerated restitution of endothelial integrity and endothelium-dependent function after phVEGF165 gene transfer. Circulation 1996;94:3291-302.

30. Walter DH, Cejna M, Diaz-Sandoval L, Willis S, Kirkwood L, Stratford PW, *et al.* Local gene transfer of phVEGF-2 plasmid by gene-eluting stents: An alternative strategy for inhibition of restenosis. Circulation 2004;110:36-45.

31. Celletti FL, Waugh JM, Amabile PG, Brendolan A, Hilfiker PR, Dake MD. Vascular endothelial growth factor enhances atherosclerotic plaque progression. Nat Med 2001;7:425-9.